Jaime J. L. Quispe, Tarcisio F. Maciel, Yuri C. B. Silva, Anja Klein, “Beamforming and link activation methods for energy efficient RIS-aided transmissions in C-RANs,” in *Proc. IEEE Global Communications Conference (Globecom)*, December 2021.

Beamforming and link activation methods for energy efficient RIS-aided transmissions in C-RANs

Jaime J. L. Quispe*, Tarcisio F. Maciel◇, Yuri C. B. Silva◇ and Anja Klein*
*Communications Engineering Lab, Technische Universität Darmstadt, Germany. Email:{j.luque, a.klein}@nt.tu-darmstadt.de
◇Wireless Telecommunications Research Group (GTEL), Federal University of Ceará, Brazil. Email:{maciel, yuri}@gtel.ufc.br

***Abstract*—This work studies the application of a reconfigurable intelligent surface (RIS) in a cloud radio access network (C-RAN) targeting the reduction of resource usage while providing adequate capacity. We investigate if an RIS can contribute to improve the trade-off between the downlink system spectral efficiency (SE) and energy consumption of a multi-base-station (BS) multi-user single-RIS setup by means of link activation, radiated power control, and operational power mode decisions that can benefit from RIS-enhanced radio channels. For this purpose, we optimize the activations jointly with BS and RIS beamforming for maximum energy efficiency (EE) under a centralized approach and subject to SE, power, fronthaul capacity, and RIS phase-shift constraints. The associated mixed-boolean non-linear problem is solved using monotonic and semidefinite relaxation methods integrated in a Branch-Reduce-and-Bound procedure. Simulations show that the RIS helps to increase the EE of a C-RAN w.r.t. its non-RIS-aided and fully-connected versions by 30% and 80%, respectively.**

***Index Terms*—Reconfigurable intelligent surfaces, energy efficiency, cell-free massive MIMO, C-RAN, beamforming, monotonic optimization, semi-definite relaxation.**

I. Introduction

Due to the growing concern about the energy efficiency (EE) of wireless networks [1], the performance of new deployments should be evaluated not only in terms of spectral efficiency (SE), but also power consumption. Cell-free multiple-input multiple-output (MIMO) implies that many base stations (BSs), thus radio-frequency (RF) chains, power amplifiers (PAs), and dedicated power-hungry digital signal processing (DSP) hardware, have to be installed for uniform coverage [2], [3], which requires a high amount of energy. The concern is well justified if we consider that, to receive 1mW of power at each user equipment (UE), up to 60W need to be generated at a power plant and up to 80% of the transmit power is lost at PAs [1], [4]. Part of these issues can be tackled by a cloud radio access network (C-RAN) which can move the power-hungry processing from the BSs to a central processing unit (CPU) to share resources and reduce hardware and power costs, as well as to increase the performance w.r.t. local processing schemes [2] and manage the fronthaul for BS coordination. However, the high amount of power spent at the PAs and other components still leaves room for improvement.

This work has been performed in the context of the LOEWE Center emergenCITY, the BMBF project Open6GHub, and has been supported by DAAD with funds from the German Federal Ministry of Education and Research (BMBF). T. F. Maciel and Y. C. B. Silva also acknowledge the support of CNPq and CAPES/PROBRAL Grant 88887.144009/2017-00.

Increasing the EE requires methods to simultaneously increase the SE and reduce the power consumption. Recently, a new class of antennas, known as reconfigurable intelligent surface (RIS), has been proposed for several wireless applications [5]–[9]. By means of electronically changing its reflection coefficients, it can reflect the incoming RF waves to desired directions without needing power-hungry components. Given its potential to tune the channels to improve the SE and power usage independently, here we investigate its benefit on the EE of a C-RAN, that, due to the mentioned reasons, is a highly suitable performance measure for this kind of networks.

Related works: An application example of RISs for EE in communication systems is the single-BS multi-UE setup [7] in which by power and RIS phase-shift optimizations a gain of 3×EE w.r.t. an Amplify-and-Forward (AF) relay scheme is reported. Minimum SE and power constraints are considered and the system is optimized by alternating between gradient descent and fractional programming (FP) steps. Subject to the same constraints, the single-BS multiple RIS setup was investigated in [8], in which in addition to BS and RIS beamforming, each optimized via successive convex approximations, RIS activations are decided via greedy search, and a 68% EE gain w.r.t. to an AF relay is reported. Also, for a practical RIS implementation, it has been studied that the configuration of the reflecting phase depends on the ability to control the impedance load of each antenna [5]. Regarding the EE of a conventional C-RAN, the work in [10] investigated the joint BS beamforming and association problem by using monotonic optimization (MO). Recently, the work in [9] studied the EE of a cell-free system with multiple RISs. The optimization is formulated as a joint power allocation and RIS phase-shift problem and it is shown that the EE can be also improved in this scenario when the radiated and BS hardware power levels are similar. In that regard, different from macrocell systems operating at kilowatt power levels, picocell BSs can be switched on or off quickly, in ms, which allows applying dynamic BS operational power control methods [1], [4]. In this work we consider a picocell-based C-RAN industrial setup in which we apply a sleep mode method assisted by an RIS to activate only the links that contribute to the EE. We use [10] as the baseline for our system model.

Scope and contributions: We investigate the contribution of an RIS to the EE performance of a C-RAN system. We noticed that there are very few other published studies on this topic besides the ones previously cited. For a multi-BS multi-UE and single-RIS setup, we optimize the link activation decisions, or equivalently BSs-UEs associations, jointly with the BS and RIS beamformers for maximum EE, which as far as we know is carried out for the first time in this work. We consider minimum SE guarantees, which is expected to be enforced but nevertheless omitted in [9]. We consider that due to hardware constraints, the RIS reflection phases can be configured within an arbitrary continuous range. We solve the optimization problem using MO and semidefinite relaxation (SDR) methods from [11] and [12]. Our solution is not rectricted to regimes or special types of beamformers as in [7] but considers the interference, as well as the DSP power consumption. For these reasons, it provides a new evaluation of the EE in RIS-aided C-RANs w.r.t. the cited studies.

Paper outline and notation: Section II addresses the system model of the RIS-aided C-RAN, including the power consumption, link activations, fronthaul capacity model, and the problem formulation. Section III presents the algorithm development together with brief descriptions of the used mathematical tools. Section IV presents the simulation setup and results and Section V concludes this paper.

The following notations are used: bold lower case, bold upper case and calligraphic letters denote vectors, matrices, and sets, respectively. $(\cdot)^{\mathrm{T}}, (\cdot)^{\mathrm{H}}, \|\cdot\|, \mathrm{diag}\,(\cdot), \arg\,(\cdot), \mathrm{tr}\,(\cdot), \Re, \Im$, denote the transpose, Hermitian, Euclidean norm, diagonal, argument, trace, real, and imaginary operators. For any two vectors $\boldsymbol{x}$ and $\boldsymbol{y} \in \mathbb{R}^N$, $\boldsymbol{x} \leq \boldsymbol{y}$ means $x_i \leq y_i$, for $i = 1, ..., N$, where x_i is the ith element of $\boldsymbol{x}$, and, unless otherwise specified, $[\boldsymbol{x}, \boldsymbol{y}]$ denotes a set or box such that for any vector $\boldsymbol{v}$ in the box, we have $\boldsymbol{x} \leq \boldsymbol{v} \leq \boldsymbol{y}$. For any set $\mathcal{V}$ and number x, $\lfloor x \rfloor_{\mathcal{V}}$ and $\lceil x \rceil_{\mathcal{V}}$ denote the floor and ceil rounded values of x on $\mathcal{V}$, whereas $\lfloor \boldsymbol{x} \rfloor_{i/\mathcal{V}}$ and $\lceil \boldsymbol{x} \rceil_{i/\mathcal{V}}$ are the corresponding vector versions that round only the ith element. $\boldsymbol{e}_i$ is the unit vector such that $e_i = 1$ and $e_j = 0, \forall j \neq i$, $\boldsymbol{A} \succeq \boldsymbol{B}$ means that $\boldsymbol{A} - \boldsymbol{B}$ is semi-definite positive, and $\mathrm{unt}\,(\boldsymbol{x})$ divides each element of $\boldsymbol{x}$ by its magnitude.

II. System Model and Problem Formulation

We consider an RIS-aided C-RAN where M BSs, each of N antennas, serve K single-antenna UEs in downlink (DL) using the same time-frequency resources via space division multiple access (SDMA). Each BS and UE is indexed by $m \in \mathcal{M} \triangleq \{1, ..., M\}$ and $k \in \mathcal{K} \triangleq \{1, ..., K\}$, respectively. One RIS of I antennas and configurable phase-shifts of unit-amplitude is available for reflecting the signals towards the intended UEs. The BSs are connected via fronthaul links to a CPU that designs the transmit strategy based on resource allocation and beamforming in a centralized way from the knowledge of the channel responses, system requirements and available resources. The configuration is then forwarded to the BSs and RIS. The data $a_k \sim \mathcal{CN}(0, 1)$ of the UE k is shared among its serving BSs. For every $k \in \mathcal{K}$ and $m \in \mathcal{M}$, $\boldsymbol{w}_{mk} \in \mathbb{C}^{N\times 1}$ is the BS beamforming vector and $\boldsymbol{d}_{mk} \in \mathbb{C}^{1\times N}$, $\boldsymbol{B}_m \in \mathbb{C}^{I\times N}$ and $\boldsymbol{q}_k \in \mathbb{C}^{1\times I}$ are the BS$_m$-UE$_k$, BS$_m$-RIS, and RIS-UE$_k$ channels, respectively. The equivalent channel for UE k is $\boldsymbol{h}_k \triangleq (\boldsymbol{d}_k + \boldsymbol{q}_k \boldsymbol{\Phi} \boldsymbol{B}) \in \mathbb{C}^{1\times MN}$ where $\boldsymbol{d}_k \triangleq [\boldsymbol{d}_{1k}, ..., \boldsymbol{d}_{Mk}]$, $\boldsymbol{B} \triangleq [\boldsymbol{B}_1, ..., \boldsymbol{B}_M]$ and $\boldsymbol{\Phi} \triangleq \mathrm{diag}\,(\boldsymbol{\phi})$ is the RIS phase-shifts matrix, where $\boldsymbol{\phi} \triangleq [e^{j\theta_1}, ..., e^{j\theta_I}]^T$ and θ_i is the phase at antenna $i \in \mathcal{I} \triangleq \{1, ..., I\}$. If $\boldsymbol{w}_k \triangleq [\boldsymbol{w}_{1k}^T, ..., \boldsymbol{w}_{Mk}^T]^T$, $\mathcal{W} \triangleq \{\boldsymbol{w}_k\}_{k\in\mathcal{K}}$, and $n_k \sim \mathcal{CN}(0, \sigma^2)$ is the noise of variance σ^2, the received signal at UE k can be modeled as

$$y_k = \boldsymbol{h}_k \boldsymbol{w}_k a_k + \sum\nolimits_{k' \in \mathcal{K}\setminus\{k\}} \boldsymbol{h}_k \boldsymbol{w}_{k'} a_{k'} + n_k, \quad (1)$$

and the signal-to-interference-plus-noise ratio (SINR) as

$$\gamma_k\,(\mathcal{W}, \boldsymbol{\phi}) = \frac{|\boldsymbol{h}_k \boldsymbol{w}_k|^2}{\sum_{k' \in \mathcal{K}\setminus\{k\}} |\boldsymbol{h}_k \boldsymbol{w}_{k'}|^2 + \sigma^2}. \quad (2)$$

Therefore, the SE of UE k is

$$r_k\,(\mathcal{W}, \boldsymbol{\phi}) = \log_2\,(1 + \gamma_k) \text{ bits/s/Hz}. \quad (3)$$

Fronthaul capacity and power consumption models: We consider the fronthaul is used to offload complex DSP from the BSs to the CPU and to share the UE DL data among the selected BSs. The link activation between BS$_m$-UE$_k$ is denoted by $x_{mk} \in \mathcal{D} \triangleq \{0, 1\}$ and the capacity c_m required by each BS m is modeled as the sum SE of the served UEs and assumed to be limited by $\overline{C}_m$, i.e.,

$$c_m = \sum\nolimits_{k\in\mathcal{K}} x_{mk} r_k \leq \overline{C}_m \text{ bits/s/Hz}, \ \forall m \in \mathcal{M}. \quad (4)$$

We consider that the total DSP power depends on c_m as

$$p_{\text{FH}} = \eta_{\text{FH}} \sum\nolimits_{m\in\mathcal{M}} c_m, \quad (5)$$

where η_{FH} is a constant factor in W/Gbits/s/Hz.

Hardware power consumption: We consider two operational modes for each BS m represented by $s_m \in \mathcal{D}$, where $s_m = 1$ indicates an active mode with power consumption $P_{\text{BS}}^{\text{run}}$ and $s_m = 0$ indicates a sleep mode with power $P_{\text{BS}}^{\text{sl}}$ [4], [10]. The power consumed by each UE and each RIS antenna is denoted by P_{UE} and P_{E}, respectively. Then, the total hardware power consumption can be modeled as

$$p_{\text{HW}} = \sum\nolimits_{m\in\mathcal{M}} (s_m P_{\text{BS}}^{\text{run}} + (1 - s_m) P_{\text{BS}}^{\text{sl}}) + K P_{\text{UE}} + I P_{\text{E}}. \quad (6)$$

Radiated power: The power used for active beamforming from BSs with PAs under constant efficiency η_{PA} is

$$p_m = \tfrac{1}{\eta_{\text{PA}}} \sum\nolimits_{k\in\mathcal{K}} \|\mathbf{w}_{mk}\|^2, \ \forall m \in \mathcal{M}, \quad (7)$$

and the radiated signal power is limited by $\overline{P}_m$, i.e.,

$$\sum\nolimits_{k\in\mathcal{K}} \|\mathbf{w}_{mk}\|^2 \leq \overline{P}_m, \ \forall m \in \mathcal{M}. \quad (8)$$

Thus, by defining $\boldsymbol{s} \triangleq \{s_m\}_{m\in\mathcal{M}}$, $\boldsymbol{x} \triangleq \{x_{mk}\}_{m\in\mathcal{M}, k\in\mathcal{K}}$, and $\boldsymbol{r} \triangleq \{r_k\}_{k\in\mathcal{K}}$, the system power consumption is given by

$$\begin{aligned} p(\boldsymbol{s}, \boldsymbol{x}, \mathcal{W}, \boldsymbol{\phi}) &= p_{\text{FH}} + p_{\text{HW}} + \sum\nolimits_{m\in\mathcal{M}} p_m \quad (9) \\ &= \eta_{\text{FH}} \sum\nolimits_{m\in\mathcal{M}} \sum\nolimits_{k\in\mathcal{K}} x_{mk} r_k\,(\mathcal{W}, \boldsymbol{\phi}) + \sum\nolimits_{m\in\mathcal{M}} s_m \Delta P + \\ &\tfrac{1}{\eta_{\text{PA}}} \sum\nolimits_{m\in\mathcal{M}} \sum\nolimits_{k\in\mathcal{K}} \|\mathbf{w}_{mk}\|^2 + P_{\text{const}}, \end{aligned}$$

where $P_{\text{const}} \triangleq M P_{\text{BS}}^{\text{sl}} + I P_{\text{E}} + K P_{\text{UE}}$ and $\Delta P \triangleq P_{\text{BS}}^{\text{run}} - P_{\text{BS}}^{\text{sl}}$.

BS activation and BS-UE associations: If UE k has guaranteed service, it should connect to at least one BS, then

$$\sum\nolimits_{m\in\mathcal{M}} x_{mk} \geq 1, \forall k \in \mathcal{K}, \tag{10}$$

and the BS m that does not serve any UE can be put into sleep mode to save energy. Then, s_m can be decided as

$$s_m = \min\left\{\sum\nolimits_{k\in\mathcal{K}} x_{mk}, 1\right\} = \max_{k\in\mathcal{K}} x_{mk},\ \forall m \in \mathcal{M}. \tag{11}$$

Problem formulation: For the given system, the maximum EE and optimal configuration problem is represented by

$$\begin{aligned}
\mathcal{P}_1 : \eta^* = \max_{\boldsymbol{\phi},\mathcal{W},\boldsymbol{x},\boldsymbol{s}} & \frac{\sum_{k\in\mathcal{K}} r_k(\mathcal{W},\boldsymbol{\phi})}{p\left(\boldsymbol{s},\boldsymbol{x},\mathcal{W},\boldsymbol{\phi}\right)} & (12)\\
\text{s.t.: } & r_k\left(\mathcal{W},\boldsymbol{\phi}\right) \geq r_o, \forall k \in \mathcal{K} & (13)\\
& \|\mathbf{w}_{mk}\|^2 \leq x_{mk}\overline{P}_m, \forall m \in \mathcal{M} & (14)\\
& \mid \phi_i \mid = 1, \forall i \in \mathcal{I} & (15)\\
& \arg\{\phi_i\} \in \mathcal{A}_i, \forall i \in \mathcal{I} & (16)\\
& \boldsymbol{s} \in \mathcal{D}^M, \boldsymbol{x} \in \mathcal{D}^{MK} & (17)\\
& (4), (8), (10), (11),
\end{aligned}$$

where η^* has the unit of bit/J/Hz. The constraints (13) are SE guarantees of r_o bits/s/Hz per UE. In (14), the BS m that is not selected by UE k $(x_{mk} = 0)$ does not need to align beams to it as well as no power is allocated to this pair. The unit-modulus and argument constraints for the RIS phase-shifts are given by (15) and (16), respectively, where $\mathcal{A}_i \triangleq [\psi_i^l, \psi_i^u] \subseteq [0, 2\pi]$ is the continuous set of phases θ_i. $\mathcal{P}_1$ is a non-convex mixed-boolean non-linear problem since 1) the utility function is not jointly concave on the variables, 2) constraints (13) and (15) are non-convex and non-linear and 3) the boolean variables $\boldsymbol{s}$ and $\boldsymbol{x}$ are mixed with continuous variables in (4), (12) and (14). $\mathcal{P}_1$ is untractable via Dinkelbach or FP transformations, however, note that (4) and (10) are explicit monotonic constraints (m.c.'s). In the next section, by using MO [11] and recent SDR methods [12], the monotonicity of $\mathcal{P}_1$ is exploited and its non-convex part is relaxed aiming to find the solution via a Branch-Reduce-and-Bound (BRnB) procedure.

III. Energy-efficient coordinated beamforming and BS-UE association via RIS

Monotonic optimization and BRnB algorithm design: Besides the non-convex mixed-boolean nature of the feasible set of $\mathcal{P}_1$, some of the constraints can be also seen as monotonic mixed-boolean and continuous, as we study below. Also, since BRnB is an optimization method that, by including monotonicity-based cuts and bounding [11], results particularly suitable for monotonic problems of large dimensions (as our C-RAN model), and can also be used over boolean sets by using boolean adjustments [11], we use it to tackle all the m.c.'s of $\mathcal{P}_1$. Also, as long as an efficient BRnB-aimed transformation can be applied to the non-convex set and subject to the existence of efficient performance bounds over the resulting region, as it is investigated in this paper, BRnB can also work on the non-convex part of $\mathcal{P}_1$ imposed by the RIS phase-shift constraints. We can unfold the hidden monotonic structure of $\mathcal{P}_1$ by replacing $\sum_{k\in\mathcal{K}}\|\mathbf{w}_{mk}\|^2$ by its epigraph $t_m, \forall m \in \mathcal{M}$, in the denominator of (12), introducing slack variables $\hat{r}_k$ in (13), $\forall k \in \mathcal{K}$, and replacing the utility function by its epigraph η_e. Also, if we replace (11) by its equivalent discrete m.c.'s (23) and (24), and replace $\hat{p}\left(\boldsymbol{s},\boldsymbol{x},\hat{\boldsymbol{r}},\boldsymbol{t}\right) = \eta_{\text{FH}} \sum_{m\in\mathcal{M}}\sum_{k\in\mathcal{K}} x_{mk}\hat{r}_k + \sum_{m\in\mathcal{M}} s_m \Delta P + \frac{1}{\eta_{\text{PA}}}\sum_{m\in\mathcal{M}} t_m + P_{\text{const}}$, the equivalent problem is then

$$\begin{aligned}
\mathcal{P}_2 : \eta^* = \max_{\eta_e,\boldsymbol{\phi},\mathcal{W},\boldsymbol{x},\boldsymbol{s},\hat{\boldsymbol{r}},\boldsymbol{t}} & \ \eta_e & (18)\\
\text{s.t.: } & \hat{r}_k \geq r_o, \forall k \in \mathcal{K}, & (19)\\
& \log_2\left(1 + \gamma_k\left(\mathcal{W},\boldsymbol{\phi}\right)\right) \geq \hat{r}_k, \forall k \in \mathcal{K}, & (20)\\
& \eta_e \hat{p}\left(\boldsymbol{s},\boldsymbol{x},\hat{\boldsymbol{r}},\boldsymbol{t}\right) - \sum\nolimits_{k\in\mathcal{K}} \hat{r}_k \leq 0, & (21)\\
& \sum\nolimits_{k\in\mathcal{K}} \|\mathbf{w}_{mk}\|^2 \leq t_m, \forall m \in \mathcal{M}, & (22)\\
& s_m \geq x_{mk}, \forall k \in \mathcal{K}, \forall m \in \mathcal{M}, & (23)\\
& s_m \leq \sum\nolimits_{k\in\mathcal{K}} x_{mk}, \forall m \in \mathcal{M}, & (24)\\
& (4), (8), (10), (14), (15), (16), (17).
\end{aligned}$$

The objective function of (18) is a monotonic increasing function (m.i.f.) on η_e. Each inequality in (4), (10), (19), (21), (23), and (24) can be expressed using either a m.i.f. or a difference of m.i.f.'s over the search set for $\boldsymbol{s}, \boldsymbol{x}, \hat{\boldsymbol{r}}$ and $\boldsymbol{t}$. Also, for the case that these variables are fixed, we can compute the objective as $\eta_e = \frac{\sum_{k\in\mathcal{K}}\hat{r}_k}{\hat{p}(\boldsymbol{s},\boldsymbol{x},\hat{\boldsymbol{r}},\boldsymbol{t})}$, and we can avoid branching on η_e. If the m.c.'s define an N_s-dimensional search set $\mathcal{S}$, with $N_s = N_d + N_c$, where $N_d = M + MK$ is the number of discrete monotonic (d.m.) variables to be optimized corresponding to $\boldsymbol{s}$ and $\boldsymbol{x}$ and $N_c = K + M$ is the number of continuous monotonic (c.m.) variables from $\hat{\boldsymbol{r}}$ and $\boldsymbol{t}$, we can define an N_t-dimensional box that contains both $\mathcal{S}$ and $\mathcal{A} \triangleq \{\mathcal{A}_i\}_{i\in\mathcal{I}}$, where $N_t = N_s + I$, such that each monotonic variable and RIS phase is represented by one vertex. If we express the inequalities involving m.i.f.'s as a single one by means of their equivalent pointwise maximum [11, Corollary 6], the monotonic structure of $\mathcal{P}_2$ can be represented as

$$\max_{\boldsymbol{v}}\ f(\boldsymbol{v}) | g(\boldsymbol{v}) \leq h(\boldsymbol{v}), \boldsymbol{v} \in [\boldsymbol{p}, \boldsymbol{q}] \subseteq \mathcal{S}, (v_1, ..., v_{N_d}) \in \mathcal{D}^{N_d},$$

where $\boldsymbol{v} \triangleq [v_1, ...v_{N_d}, v_{N_d+1}, ..., v_{N_s}]^T$ is composed of the d.m. and c.m. variables, whose lower and upper bounds are given by $\boldsymbol{p} \triangleq [\underline{\boldsymbol{s}}^T, \underline{\boldsymbol{x}}^T, \underline{\hat{\boldsymbol{r}}}^T, \underline{\boldsymbol{t}}^T]^T$ and $\boldsymbol{q} \triangleq [\overline{\boldsymbol{s}}^T, \overline{\boldsymbol{x}}^T, \overline{\hat{\boldsymbol{r}}}^T, \overline{\boldsymbol{t}}^T]^T$, respectively, and $g(\boldsymbol{v})$ and $h(\boldsymbol{v})$ are m.i.f.'s on $\boldsymbol{v}$.

Branching: At each iteration, the chosen box $B = [\boldsymbol{p}, \boldsymbol{q}]$, is divided on its longest edge $n = \arg\max_{m=1,...,N_s}\left(q_m - p_m\right)$, s.t. $d = \left(q_n - p_n\right)/2$, into boxes B_- and B_+ as

$$B_- = \begin{cases} [\boldsymbol{p}, \lfloor \boldsymbol{q} - d\boldsymbol{e}_n \rfloor_{n/\mathcal{D}}], & \text{if } n \leq N_d, \\ [\boldsymbol{p}, \boldsymbol{q} - d\boldsymbol{e}_n], & \text{if } N_d < n \leq N_s, \end{cases} \tag{25}$$

$$B_+ = \begin{cases} [\lceil \boldsymbol{p} + d\boldsymbol{e}_n \rceil_{n/\mathcal{D}}, \boldsymbol{q}], & \text{if } n \leq N_d, \\ [\boldsymbol{p} + d\boldsymbol{e}_n, \boldsymbol{q}], & \text{if } N_d < n \leq N_s. \end{cases}$$

Reduction: at each iteration, we remove points of $B = [\boldsymbol{p}, \boldsymbol{q}]$, that are not in $\mathcal{S}$, and achieve a local performance below the best global η_e^{global} obtained until that iteration, while not losing any optimal solution in B [11]. We represent the reduction as $f_r : B \to B'$, which returns a reduced box $B' = [\boldsymbol{p}', \boldsymbol{q}'] \subset B$ containing points $\boldsymbol{v} \in [\boldsymbol{p}, \boldsymbol{q}] \cap \mathcal{S}$ s.t. $f(\boldsymbol{v}) > \eta_e^{global}$ if $g(\boldsymbol{p}) \le h(\boldsymbol{q})$, and if $\boldsymbol{p}' = \boldsymbol{q} - \sum_{n=1}^{N_s} \alpha_n (q_n - p_n)\boldsymbol{e}_n$ and $\boldsymbol{q}' = \boldsymbol{p} - \sum_{n=1}^{N_s} \beta_n (p_n - q_n)\boldsymbol{e}_n$, where $\alpha_n = \sup\{\alpha | 0 \le \alpha \le 1,\ g(\boldsymbol{p}) \le h(\boldsymbol{q} - \alpha(q_n - p_n)\boldsymbol{e}_n), f(\boldsymbol{q} - \alpha(q_n - p_n)\boldsymbol{e}_n) \ge \eta_e^{global}\}$ and $\beta_n = \sup\{\beta | 0 \le \beta \le 1,\ g(\boldsymbol{p} - \beta(p_n - q_n)\boldsymbol{e}_n) \le h(\boldsymbol{q}), f(\boldsymbol{q}) \ge \eta_e^{global}\}$. We compute α_n and β_n for every $n = 1, ..., N_s$, via bisection.

Boolean adjustment: For each $n \le N_d$, p'_n and q'_n are replaced by $\lceil p'_n \rceil_{\mathcal{D}}$ and $\lfloor q'_n \rfloor_{\mathcal{D}}$, respectively.

Bounding: Although $\eta_e(\boldsymbol{v})$ is not a m.i.f. on $\boldsymbol{v}$, local lower bound (l.b.) and upper bound (u.b.) can be still computed from the monotonicity of its numerator and denominator as

$$\eta_e^{llb}(B) = \frac{\sum_{k\in\mathcal{K}} \underline{\hat{r}_k}}{\hat{p}\left(\overline{\boldsymbol{s}}, \overline{\boldsymbol{x}}, \overline{\hat{\boldsymbol{r}}}, \overline{\boldsymbol{t}}\right)}, \quad \eta_e^{lub}(B) = \frac{\sum_{k\in\mathcal{K}} \overline{\hat{r}_k}}{\hat{p}\left(\underline{\boldsymbol{s}}, \underline{\boldsymbol{x}}, \underline{\hat{\boldsymbol{r}}}, \underline{\boldsymbol{t}}\right)}. \quad (26)$$

Note that we use both lower and upper corners of B. At each iteration i, we reduce the search space by removing the boxes that provide a local u.b. for η_e below the best global l.b., i.e. B is discarded if $\eta_e^{\text{lub}}(B) < \eta_{e,i}^{\text{glb}}$ and also the global bound can be updated as $\eta_{e,i}^{glb} = \max(\eta_{e,i-1}^{glb}, \eta_e^{llb}(B))$.

First, we define an initial N_t-dimensional box $B_0 \supseteq \mathcal{S} \cup \{\mathcal{A}_i\}_{i\in\mathcal{I}}$ as $B_0 \triangleq [\boldsymbol{p}, \boldsymbol{q}]$ with I vertices for the RIS phases $\boldsymbol{\theta}$. We can initialize $\underline{s}_m = 0, \overline{s}_m = 1, \underline{x}_{mk} = 0, \overline{x}_{mk} = 1, \underline{t}_m = 0, \overline{t}_m = \overline{P}_m, \underline{\hat{r}}_k = r_o, \overline{\hat{r}}_k = \max\{\overline{C}_m\}_{m\in\mathcal{M}}, \underline{\theta}_i = \varphi_i^l$ and $\overline{\theta}_i = \varphi_i^u$. Then, B_0, and henceforth in general a box B, is branched and reduced to B'. Next, the search of feasible solutions for $\mathcal{W}$ and $\boldsymbol{\phi}$ in the region defined by (8), (14), (15), (16), (20) and (22) shaped by the corners of B' is the problem

$$\begin{aligned}\mathcal{P}_3 :&\{\mathcal{W}_B, \boldsymbol{\phi}_B\} = \text{find } \{\mathcal{W}, \boldsymbol{\phi}\}\\ \text{s.t.:}&\sum_{k\in\mathcal{K}} \|\mathbf{w}_{mk}\|^2 \le \min\{\overline{P}_m, t_m\}, \forall m \in \mathcal{M}, \quad (27)\\ &\{(14), (15), (16), (20)\} \cap f_r(B),\end{aligned}$$

where (27) is the convex intersection of (8) and (22). If $\{\mathcal{W}_B, \boldsymbol{\phi}_B\} \ne \emptyset$, the local l.b. and u.b. of η_e can be computed with (26). However, certifying the feasibility of $\mathcal{P}_3$ is not trivial due to its non-convex constraints (15), (16) and (20). In this case, $\mathcal{P}_3$ can be tackled as an optimization problem and we consider the minimization of the radiated signal power as

$$\begin{aligned}\mathcal{P}_4 :&\{\mathcal{W}_B^*, \boldsymbol{\phi}_B^*\} = \min_{\mathcal{W}, \boldsymbol{\phi}} \sum_{m\in\mathcal{M}} \sum_{k\in\mathcal{K}} \|\mathbf{w}_{mk}\|^2 \quad (28)\\ &\text{s.t.:}\{(14), (15), (16), (20), (27)\} \cap f_r(B).\end{aligned}$$

Since $\mathcal{P}_2$ is subject to power, SE and fronthaul constraints and of these only the two first are in $\mathcal{P}_4$, we check that

$$\sum_{k\in\mathcal{K}} \underline{\hat{r}}_k \le \sum_{m\in\mathcal{M}} \overline{s}_m \overline{C}_m, \quad (29)$$

before solving $\mathcal{P}_4$ which is due to $\sum_{m\in\mathcal{M}} \overline{s}_m \overline{C}_m \ge \sum_{m\in\mathcal{M}} \sum_{k\in\mathcal{K}} x_{mk} \hat{r}_k \ge \sum_{k\in\mathcal{K}} \hat{r}_k \sum_{m\in\mathcal{M}} x_{mk} \ge \sum_{k\in\mathcal{K}} \underline{\hat{r}}_k$. If (29) does not hold, B does not contain any feasible solution and we can discard it. $\mathcal{P}_4$ can be solved alternately on $\mathcal{W}$ and $\boldsymbol{\phi}$. The optimization is performed over the convex expansion of the RIS phase set $\mathcal{A}$ aiming to ease the feasibility check of $\mathcal{P}_3$, i.e., if there is no feasible point in the expanded region, over which $\mathcal{P}_4$ can be solved, it means there is also no solution within the original smaller set. This relaxation provides us an optimistic l.b. for $\boldsymbol{t}$ that we can use to compute new local bounds for η_e. For fixed $\boldsymbol{\phi}$, $\mathcal{P}_4$ reduces to

$$\mathcal{P}_5 : \mathcal{W}_B^* = \min_{\mathcal{W}} \sum_{m\in\mathcal{M}} \sum_{k\in\mathcal{K}} \|\mathbf{w}_{mk}\|^2, \text{ s.t.:} \quad (30)$$

$$\boldsymbol{h}_k \boldsymbol{w}_k \ge \sqrt{\underline{\gamma_k} \sum_{k'\in\mathcal{K}\setminus\{k\}} (|\boldsymbol{h}_k \boldsymbol{w}_{k'}|^2 + \sigma^2)}, \forall k, \quad (31)$$

$$\Im(\boldsymbol{h}_k \boldsymbol{w}_k) = 0, \forall k, \quad (32)$$

$$\|\mathbf{w}_{mk}\|^2 \le \overline{x}_{mk} \overline{P}_m, \forall m, \forall k, \quad (33)$$

$$\underline{s}_m \underline{t}_m \le \sum_{k\in\mathcal{K}} \|\mathbf{w}_{mk}\|^2 \le \overline{s}_m \min\{\overline{P}_m, \overline{t}_m\}, \forall m, \quad (34)$$

where $\underline{\gamma_k} \triangleq 2^{\underline{\hat{r}_k}} - 1$ is the SINR corresponding to $\underline{\hat{r}_k}$ and $\boldsymbol{h}_k = \boldsymbol{d}_k + \boldsymbol{q}_k \text{diag}(\boldsymbol{\phi})\boldsymbol{B}$ is the combined channel from all BSs to UE k via the RIS. Then, for fixed $\mathcal{W}$, $\mathcal{P}_4$ reduces to

$$\begin{aligned}&\mathcal{P}_6 : \boldsymbol{\phi}_B^* = \text{find } \boldsymbol{\phi}, \text{ s.t.:}\\ &\frac{|\bar{d}_{kk} + \boldsymbol{\phi}^T \bar{\boldsymbol{b}}_{kk}|^2}{\sum_{k'\ne k} |\bar{d}_{kk'} + \boldsymbol{\phi}^T \bar{\boldsymbol{b}}_{kk'}|^2 + \sigma_k^2} \ge 2^{\underline{\hat{r}_k}} - 1, \forall k \in \mathcal{K}, \quad (35)\\ &(15), (16),\end{aligned}$$

where $\bar{d}_{kk'} = \boldsymbol{d}_k \boldsymbol{w}_{k'} \in \mathbb{C}$ and $\bar{\boldsymbol{b}}_{kk'} = \text{diag}(\boldsymbol{q}_k)\boldsymbol{B}\boldsymbol{w}_{k'}$. For every $k \in \mathcal{K}$, (35) can be transformed to the quadratic form $\boldsymbol{v}^H \boldsymbol{R}_{kk} \boldsymbol{v} + |\bar{d}_{kk}|^2 \ge \underline{\gamma}_k \sum_{k\in\mathcal{K}\setminus\{k'\}} (\boldsymbol{v}^H \boldsymbol{R}_{kk'} \boldsymbol{v} + |\bar{d}_{kk'}|^2 + \sigma_k^2)$, where $\boldsymbol{R}_{kk'} \triangleq \begin{bmatrix} \bar{\boldsymbol{b}}_{\boldsymbol{kk'}} \bar{\boldsymbol{b}}_{\boldsymbol{kk'}}^H & \bar{\boldsymbol{b}}_{\boldsymbol{kk'}} \bar{d}_{kk'}^* \\ \bar{d}_{kk'} \bar{\boldsymbol{b}}_{\boldsymbol{kk'}}^H & 0 \end{bmatrix}$ and $\boldsymbol{v} \triangleq [\boldsymbol{\phi}^T, 1]^T$ is an auxiliary variable [6]. Aiming at faster convergence of $\mathcal{P}_4$, the power achieved in $\mathcal{P}_5$ can be further reduced by minimizing the SINR residuals in (31) via auxiliary variables α_k. If $\boldsymbol{V} \triangleq \boldsymbol{v}\boldsymbol{v}^H$, $\mathcal{P}_6$ can be reformulated as

$$\mathcal{P}_7 : \{\boldsymbol{v}_B, \boldsymbol{V}_B\} = \max_{\boldsymbol{v}, \boldsymbol{V}\succeq 0, \boldsymbol{\alpha}} \sum_{k\in\mathcal{K}} \alpha_k \quad (36)$$

$$\begin{aligned}\text{s.t.: } &\text{tr}(\boldsymbol{R}_{kk}\boldsymbol{V}) + |\bar{d}_{kk}|^2 \ge \underline{\gamma}_k \sum_{k'\ne k} \text{tr}(\boldsymbol{R}_{kk'}\boldsymbol{V}) +\\ &\underline{\gamma}_k (\sum_{k'\ne k} |\bar{d}_{kk'}|^2 + \sigma_k^2) + \alpha_k, \forall k \in \mathcal{K}, \quad (37)\\ &\boldsymbol{V} = \boldsymbol{v}\boldsymbol{v}^H, \quad (38)\\ &\boldsymbol{V}_{ii} = 1, i = 1, ..., I+1, \quad (39)\\ &\arg(v_i) \in \mathcal{V}_i^B, \forall i \in \mathcal{I}, \quad (40)\\ &v_{I+1} = 1, \quad (41)\\ &\alpha_k \ge 0, \forall k \in \mathcal{K}, \quad (42)\end{aligned}$$

where $\mathcal{V}_i^B \triangleq [l_i^B, u_i^B] \in [0, 2\pi], \forall i \in \mathcal{I}$ is the search set for the argument of v_i in box B with lower and upper corners l_i and u_i, respectively. Note that a solution for $\boldsymbol{\phi}$ can be recovered directly from $\boldsymbol{v}_B$. We conveniently map the initial search sets $\mathcal{A}_i$ to $\mathcal{V}_i$ as $l_i = (2\pi - \psi_i^u)$ and $u_i = (2\pi - \psi_i^l), \forall i \in \mathcal{I}$, for the purpose of branching over $\arg(v_i)$, i.e., $\arg(v_i)$ are the vertices to be included in $\mathcal{B}_0$. The convexity of $\mathcal{P}_7$ is prevented by the rank-one condition in (38). By dropping it, $\mathcal{P}_7$ gets independent of $\boldsymbol{v}$, thus can be tackled via SDP and an approximate solution for $\boldsymbol{v}_B$ can be extracted from $\boldsymbol{V}_B$, e.g., via eigenvalue decomposition or randomization methods [13], [14]. However, it is not guaranteed that the obtained $\boldsymbol{v}_B$ meets (40). A common method is dropping (40), however this might cause feasible solutions to be lost. Therefore, instead of it, we replace these constraints by semidefinite and linear inequalities, respectively, derived from a tight convex expansion of $\{\mathcal{V}_i^B\}_{i\in\mathcal{I}}$ as follows.

Enhanced SDP relaxation: For each box B, omitting the superscripts, the arc on each argument set $\mathcal{V}_i \triangleq [l_i, u_i] \subset [0, 2\pi]$ can be expanded to its circular segment as $\mathcal{V}_i' = \{v_i \in \mathbb{C} \mid \Re(a_i^* v_i) \geq \cos(\frac{u_i - l_i}{2}), |v_i| \leq 1\}$, where $a_i \triangleq e^{\frac{u_i + l_i}{2}}, \forall i \in \mathcal{I}$ [12]. Also, $|v_i| \leq 1$ can be realized implicitly by relaxing (38) to $\boldsymbol{V} \succeq \boldsymbol{v}\boldsymbol{v}^H$. Then $\mathcal{P}_7$ can be reformulated as

$$\mathcal{P}_8 : \{\tilde{\boldsymbol{v}}_B, \tilde{\boldsymbol{V}}_B\} = \max_{\boldsymbol{v}, \boldsymbol{V}\succeq 0, \boldsymbol{\alpha}} \sum\nolimits_{k\in\mathcal{K}} \alpha_k \tag{43}$$

$$\text{s.t.: } \boldsymbol{V} \succeq \boldsymbol{v}\boldsymbol{v}^H \tag{44}$$

$$\Re(a_i^* v_i) \geq \cos(\tfrac{u_i^B - l_i^B}{2}), \forall i \in \mathcal{I}, \tag{45}$$

$$(37), (39), (41), (42).$$

The new introduced constraints (44) and (45) enable solving $\mathcal{P}_8$ straightforwardly with an SDP solver. Then, the solvers for $\mathcal{P}_5$ and $\mathcal{P}_8$ can be alternated, as long as $\text{rank}(\boldsymbol{H}) \geq K$, with $\boldsymbol{H} \triangleq [\boldsymbol{h}_1^T, ..., \boldsymbol{h}_K^T]$. Branching over $\arg(v_i)$ is based on the fact that if for each vertex i, the width of $\mathcal{V}_i$: $(u_i - l_i) \to 0 \Rightarrow |v_i| \to 1$, for any feasible solution v_i within $\mathcal{V}_i'$. Also, if $\tilde{\boldsymbol{v}}$ is the feasible solution of $\mathcal{P}_8$, with $|\tilde{v}_i| = 1, \forall i \in \mathcal{I}$, then $\tilde{\boldsymbol{v}}$ is also feasible for $\mathcal{P}_7$ [12]. That means that $\mathcal{V}$ has to be sucessively branched across BRnB iterations in order to move $\tilde{\boldsymbol{v}}$, thus $\boldsymbol{\phi}$, towards the circle contour, i.e., satisfying (15) and (16). Therefore, in the selection of the longest edge for branching box B into B_- and B_+, the candidate among the edges $n = N_s + 1, ..., N_t$, is the phase i given by $i_{\max} = \arg\max_{i\in\mathcal{I}}\{|\text{unt}(\tilde{v}_i) - \tilde{v}_i|\}$, i.e., this length is compared with those of the vertices of the monotonic variables. If $\mathcal{W}^*$ is the solution of the relaxed $\mathcal{P}_4$, $\tilde{\boldsymbol{t}}$, with $\tilde{t}_m = \sum_{k\in\mathcal{K}} \|\mathbf{w}_{mk}^*\|^2$, can be interpreted as the optimistic minimum power required to achieve $\hat{\underline{\boldsymbol{r}}}$, i.e., $\underline{\boldsymbol{t}} \leq \tilde{\boldsymbol{t}} \leq \boldsymbol{t}^*$, where $\boldsymbol{t}^*$ represents the exact optimal minimum power. Therefore, as a l.b. for $\boldsymbol{t}$, $\tilde{\boldsymbol{t}}$ is tighter than $\underline{\boldsymbol{t}}$. If we replace $\underline{\boldsymbol{t}}$ by $\tilde{\boldsymbol{t}}$, 1) branching over $\boldsymbol{t}$ can be skipped, and 2) a new u.b. for η_e tighter than η_e^{lub} in (26) can be computed. For this purpose, a new l.b. for $\hat{p}(\boldsymbol{s}, \boldsymbol{x}, \hat{\boldsymbol{r}}, \boldsymbol{t})$ over box B can be computed as

$$\underline{\hat{p}}(\underline{\boldsymbol{s}}, \underline{\boldsymbol{x}}, \hat{\underline{\boldsymbol{r}}}, \tilde{\boldsymbol{t}}) = \tfrac{1}{\eta_{\text{PA}}} \sum\nolimits_{m\in\mathcal{M}} \tilde{t}_m + \Delta P \max(1, \sum\nolimits_{m\in\mathcal{M}} \underline{s}_m) + \eta^{\text{FH}} \max(\sum\nolimits_{k\in\mathcal{K}} \underline{\hat{r}}_k, \sum\nolimits_{m\in\mathcal{M}} \sum\nolimits_{k\in\mathcal{K}} \underline{x}_{mk} \underline{\hat{r}}_k) + P_{\text{const}}, \tag{46}$$

where the first term comes from the optimistic SDR solution of $\mathcal{P}_5$, the second is because at least one BS should be enabled to serve the UEs, and the third is due to (10), and $\sum_{m\in\mathcal{M}} \sum_{k\in\mathcal{K}} x_{mk} r_k \geq \sum_{k\in\mathcal{K}} r_k$. Since $\underline{\hat{p}}(\underline{\boldsymbol{s}}, \underline{\boldsymbol{x}}, \hat{\underline{\boldsymbol{r}}}, \tilde{\boldsymbol{t}}) \geq \hat{p}(\underline{\boldsymbol{s}}, \underline{\boldsymbol{x}}, \hat{\underline{\boldsymbol{r}}}, \underline{\boldsymbol{t}})$, a new local u.b. for η_e is given by

$$\underline{\eta}_e^{lub}(B) = \frac{\sum_{k\in\mathcal{K}} \overline{\hat{r}_k}}{\underline{\hat{p}}(\underline{\boldsymbol{s}}, \underline{\boldsymbol{x}}, \hat{\underline{\boldsymbol{r}}}, \tilde{\boldsymbol{t}})} \leq \eta_e^{lub}. \tag{47}$$

The local bound η_e^{llb}, which is based on monotonicity, can be improved via any feasible solution of $\mathcal{P}_2$, say $\bar{\boldsymbol{v}} \triangleq (\tilde{\boldsymbol{s}}, \tilde{\boldsymbol{x}}, \hat{\underline{\boldsymbol{r}}}, \tilde{\boldsymbol{t}}) \in B$, as long as it can be obtained, otherwise we can still compute η_e^{llb} using (26). We use the heuristic in [10] to find a candidate point $\tilde{\boldsymbol{x}}$ from $\mathcal{W}^*$ as $\tilde{x}_{mk} = 1$ if $\|\mathbf{w}_{mk}^*\| > 0$, and $\tilde{x}_{mk} = 0$ if $\|\mathbf{w}_{mk}^*\| = 0$ and if it meets (4) and (10), thus the minimum rate $\hat{\underline{\boldsymbol{r}}}$ in B, from (11), we have $\tilde{s}_m = \max_{k\in\mathcal{K}} \tilde{x}_{mk}$ and a new l.b. on B can be computed as

$$\overline{\eta}_e^{llb}(B) = \frac{\sum_{k\in\mathcal{K}} \underline{\hat{r}}_k}{\underline{\hat{p}}(\tilde{\boldsymbol{s}}, \tilde{\boldsymbol{x}}, \hat{\underline{\boldsymbol{r}}}, \tilde{\boldsymbol{t}})} \geq \eta_e^{llb}. \tag{48}$$

The steps for solving $\mathcal{P}_1$ are summarized in Algorithm 1. The convergence is guaranteed since at each iteration we check the l.b. provided by each of the two descendant boxes and update $\eta_{e,i}^{\text{glb}}$ only when a higher l.b. is found and also since η_e is upper-bounded by capacity and power constraints. We can claim only probable optimality since $\mathcal{P}_4$ is not jointly convex on $\mathcal{W}$ and $\boldsymbol{\phi}$ and we use an alternating method to compute $\tilde{\boldsymbol{t}}$.

IV. Numerical Results

We consider an example setup of 2 three-antenna BSs, 3 single-antenna UEs and a four-antenna RIS in LoS of the BSs, i.e. $M = 2, N = 3, K = 3$ and $I = 4$. We assume uniform-linear antenna arrays (ULAs) with half-wavelength spacing at the RIS and each BS. The BS_m-RIS, BS_m-UE_k, and RIS-UE_k channel path losses are β_m^B, β_{mk}^d, and β_k^q, respectively, and follow the 3GPP Urban Micro parameters in [15, Table B.1.2.1-1] at 2.5 GHz. We use the LoS version plus Rician fading for the BS-RIS channel and the NLoS version plus Rayleigh fading for the rest. The channels are given by $\boldsymbol{B}_m = \sqrt{\beta_m^B}\left(\sqrt{\rho_m^B/(\rho_m^B + 1)}\bar{\boldsymbol{B}}_m + \sqrt{1/(\rho_m^B + 1)}\tilde{\boldsymbol{B}}_m\right)$, $\boldsymbol{q}_k = \sqrt{\beta_k^q}\tilde{\boldsymbol{q}}_k$ and $\boldsymbol{d}_{mk} = \sqrt{\beta_{mk}^d}\tilde{\boldsymbol{d}}_{mk}$, where the elements of the NLOS components $\tilde{\boldsymbol{B}}_m$, $\tilde{\boldsymbol{q}}_k$ and $\tilde{\boldsymbol{d}}_{mk}$ follow $\mathcal{CN}(0, 1)$. The ULA response is $\alpha_N(\Omega) = \left[1, e^{j\pi\sin\Omega}, ..., e^{j\pi(N-1)\sin\Omega}\right]$ and $\bar{\boldsymbol{B}}_m = \alpha_I(\Omega_{AoA,m})\,\alpha_N(\Omega_{AoD,m})^H$, where $\Omega_{AoA,m}$ is the AoA at the RIS from BS m and $\Omega_{AoD,m}$ is the AoD at the BS m to the RIS. We assume an inter-BS distance of 200m, UEs randomly positioned in an area of 400m^2, $\sigma^2 = -126$dBW, $r_o = 3$bits/s/Hz, $P_{\text{E}} = 10$mW, $P_{\text{UE}} = 0.1$W, $\varphi_i^l = \frac{3\pi}{2}$ and $\varphi_i^u = 2\pi, \forall i$. For both BSs, $\rho_m^B = 10$, $\overline{P}_m = 0.25$W, $\overline{C}_m = 10$bits/s/Hz, $P_{\text{BS}}^{\text{run}} = 10$W, $P_{\text{BS}}^{\text{sl}} = 2$W, $\eta_{\text{PA}} = 0.25$ and $\eta_{\text{FH}} = 0.2$. Algorithm precision $\epsilon_1 = 10^{-4}, \epsilon_2 = \epsilon_3 = 10^{-5}$. We consider two benchmarks. The first is a non-RIS aided C-RAN (baseline) that is optimized for EE using a variant of Algorithm 1, derived from considering only the direct channels $\boldsymbol{d}_k$ and solving the auxiliary $\mathcal{P}_4$ as a second-order cone problem since the RIS-related constraints can be omitted. The second is a fully connected system (C-RAN full-connection) also optimized by Algorithm 1 with fixed $s_m = 1$ and $x_{mk} = 1, \forall m, k$. The system parameters are kept the same for the benchmarks. For one channel realization, Fig.1 presents the convergence of Algorithm 1 for our RIS C-RAN setup as well as for the benchmarks using their respective lower and upper bounds for η^*. We see that the bounds converge to the optimal value along the iterations and RIS

Algorithm 1: BRnB algorithm for solving $\mathcal{P}_1$

Result: $\eta^*, \boldsymbol{\phi}, \mathcal{W}, \boldsymbol{x}, \boldsymbol{s}$
initialize $B_0 = [\boldsymbol{p}, \boldsymbol{q}]$ for $\boldsymbol{s}, \boldsymbol{x}, \hat{\boldsymbol{r}}, \boldsymbol{t}$ and $\arg(\boldsymbol{v})$, the box set $\mathcal{B}_0 = f_r(B_0)$, $\eta_e^{glb} = 0$ and iteration index $i = 1$
while $(\eta_{e,i}^{gub} - \eta_{e,i}^{glb})/\eta_{e,i}^{gub} > \epsilon_1$ **do**
  select box $B = \arg\max_{b \in \mathcal{B}_{i-1}} \eta_e^{lub}(b)$
  select edge $n = \arg\max_{m=1,\ldots,N_t} (q_m - p_m)$ giving priority to $\boldsymbol{s}$ until $\underline{\boldsymbol{s}} = \overline{\boldsymbol{s}}$ and branch B into B_1 and B_2 using (25)
  for $r = 1 : 2$ **do**
    reduce B_r to B'_r via bisection with precision ϵ_2, discard it if reduction is infeasible
    if B'_r *meets* (29) **then**
      if *optimistic* $\eta_e^{lub}(B'_r) > \eta_e^{glb}$ **then**
        initialize $\boldsymbol{\phi} = e^{j(\underline{\boldsymbol{\theta}} + \overline{\boldsymbol{\theta}})/2}$ and $l = 0$
        repeat solve $\mathcal{P}_5$ for fixed $\boldsymbol{\phi}^l$ and get $\mathcal{W}^l$
          solve $\mathcal{P}_7$ for fixed $\mathcal{W}^l$ and get $\boldsymbol{\phi}^l$
          $l \leftarrow l + 1$
        until *relative decrease of power* $\geq \epsilon_3$ *or* $\mathcal{P}_7$ *is infeasible*
        if *infeasible* **then** discard B'_r
        else
          obtain $\tilde{\boldsymbol{t}}$, $\mathcal{W}^*$, $\boldsymbol{\phi}^*$
          update vertices $\underline{\boldsymbol{t}} \leftarrow \tilde{\boldsymbol{t}}$ in B'_r
          compute $\eta_e^{lub}(B'_r)$ using (47)
          compute point $\bar{\boldsymbol{v}}$ and check (4) (10)
          if *candidate* $\bar{\boldsymbol{v}}$ *is feasible* **then**
            compute $\overline{\eta}_e^{llb}(\boldsymbol{v})$, (48)
            $\eta_e^{llb}(B'_r) \leftarrow \overline{\eta}_e^{llb}(\boldsymbol{v})$
          else compute $\eta_e^{llb}(B'_r)$ using (26).
          update $\eta_{e,i}^{glb} = \max(\eta_{e,i-1}^{glb}, \eta_e^{llb}(B'_r))$
      else discard B'_r, new optimal is not here
    else discard B'_r, no feasible points
  update set $\mathcal{B}_i \leftarrow (\mathcal{B}_{i-1} \setminus B) \cup \{B'_r | \eta_e^{lub}(B'_r) \geq \eta_{e,i}^{glb}\}$
  update $\eta_{e,i}^{gub} = \max_{b \in \mathcal{B}_i}(\eta_e^{lub}(b))$ and $i \leftarrow i + 1$.

C-RAN is more energy efficient than the two benchmarks in 30% and 80%, respectively. This is due to better link activation decisions and beamformers are obtained with the RIS channels and less power is needed to be transmitted from the BSs, i.e. each term p_m in (9) was reduced. The fully connected case has the lowest EE since it is the most affected by interference. Also, by using the SDR-based lower and upper bounds for η_e, the algorithm converges faster for the RIS case and it might be due to a larger degree of freedom provided by the RIS to search the beamformers. Further simulations on different channel realizations showed that the BS cooperation can be relaxed and only one BS needs to be active whereas the second can be put into sleep mode, which saves energy equivalent to ΔP, as well as the SEs can be increased w.r.t. the benchmarks.

V. Conclusion

We investigated the benefits of RIS signal reflections in EE of C-RANs composed of multiple BSs and UEs subject to SE, power and capacity constraints. By using MO and SDR methods, we optimized the link activations and the BS and RIS beamformers for maximum energy efficiency to reduce the radiated and operational BS power while providing adequate SE. In simulation, we observed an EE in bits/J/Hz 30% and 80% higher than in its non-RIS activation-optimized and fully-connected versions, respectively.

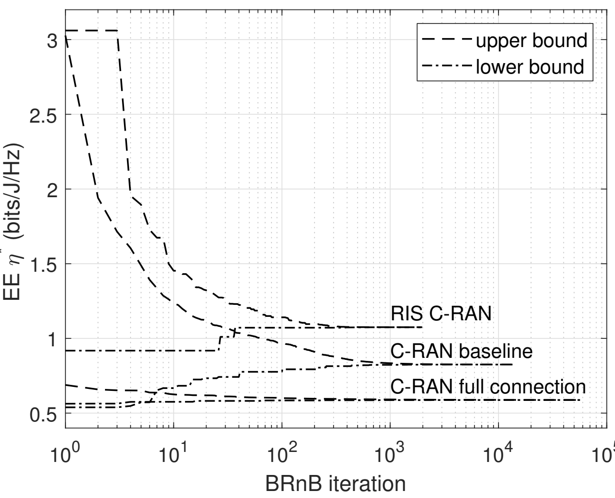

Fig. 1. Energy Efficiency Optimization using Algorithm 1

References

[1] B. Zahnstecher, "The 5G Energy Gap [Expert View]," *IEEE Power Electron. Mag.*, Vol. 6, No. 4, pp. 64-67, 2019.

[2] E. Björnson and L. Sanguinetti, "Making Cell-Free Massive MIMO Competitive With MMSE Processing and Centralized Implementation," *IEEE Trans. Wireless Commun.*, Vol. 19, No. 1, pp. 77-90, 2020.

[3] G. Interdonato, P. Frenger and E. Larsson, "Scalability Aspects of Cell-Free Massive MIMO," *IEEE Int. Conf. on Commun.*, pp. 1-6, 2019.

[4] I. Ashraf, F. Boccardi, and L. Ho, "SLEEP mode techniques for small cell deployments," *IEEE Commun. Mag.*,Vol. 49, No. 8, pp. 72-79, 2011.

[5] A. Pitilakis et al., "A Multi-Functional Reconfigurable Metasurface: Electromagnetic Design Accounting for Fabrication Aspects," *IEEE Trans. Antennas Propag.*, Vol. 69, No. 3, pp. 1440-1454, 2021.

[6] Q. Wu and R. Zhang, "Intelligent Reflecting Surface Enhanced Wireless Network via Joint Active and Passive Beamforming," *IEEE Trans. Wireless Commun.*, Vol. 18, No. 11, pp. 5394-5409, 2019.

[7] C. Huang, A. Zappone, G. C. Alexandropoulos, M. Debbah and C. Yuen, "Reconfigurable Intelligent Surfaces for Energy Efficiency in Wireless Communication," *IEEE Trans. Wireless Commun.*, Vol. 18, No. 8, pp. 4157-4170, 2019.

[8] Z. Yang, *et al.*, "Energy-Efficient Wireless Communications with Distributed Reconfigurable Intelligent Surfaces," 2020, *arXiv:2005.00269*.

[9] Y. Zhang et al., "Beyond Cell-free MIMO: Energy Efficient Reconfigurable Intelligent Surface Aided Cell-free MIMO Communications," *IEEE Trans. Cogn. Commun. Netw.*, 2021.

[10] K. Nguyen, Q. Vu, M. Juntti and L. Tran, "Energy Efficiency Maximization for C-RANs: Discrete Monotonic Optimization, Penalty, and ℓ_0-Approximation Methods," *IEEE Trans. Signal Process.*, Vol. 66, No. 17, pp. 4435-4449, 2018.

[11] H. Tuy, M. Minoux and N. Hoai-Phuong, "Discrete Monotonic Optimization with Application to a Discrete Location Problem," *SIAM J. Optim.*, Vol. 17, No. 1, pp. 78-97, 2006.

[12] L. Cheng, D. Zhibin, W. Zhang and S. Fang, "Argument division based branch-and-bound algorithm for unit-modulus constrained complex quadratic programming," *J. Glob. Optim.*, Vol. 70, No. 1, pp. 171-187, 2018.

[13] A. So, J. Zhang, and Y. Ye, "On approximating complex quadratic optimization problems via semidefinite programming relaxations," *Math. Program.*, Vol. 110, No. 1, pp. 93–110, 2007.

[14] Z. Luo, W. Ma, A. So, Y. Ye and S. Zhang, "Semidefinite Relaxation of Quadratic Optimization Problems," *IEEE Signal Process. Mag.*, Vol. 27, No. 3, pp. 20-34. 2010.

[15] 3GPP, *Further advancements for E-UTRA physical layer aspects (Release 9)*, 3GPP TS 36.814, Mar. 2017.